Probing the Plasticity in the Active Site of Protein N-terminal Methyltransferase 1 Using Bisubstrate Analogs

Dongxing Chen[†], Cheng Dong[§], Guangping Dong[†], Karthik Srinivasan[‡], Jinrong Min[§], Nicholas Noinaj[‡], and Rong Huang[†,]*

[†]Department of Medicinal Chemistry and Molecular Pharmacology, Center for Cancer Research, Institute for Drug Discovery, Purdue University, West Lafayette, Indiana 47907, United States.

[§]Structural Genomics Consortium, Department of Physiology, University of Toronto, Toronto, Ontario, Canada.

[‡]Markey Center for Structural Biology, Department of Biological Sciences and the Purdue Institute of Inflammation, Immunology and Infectious Disease, Purdue University, West Lafayette, Indiana 47907, United States.

* Correspondence should be addressed to R.H. (huang-r@purdue.edu)

Abstract: The interactions of a series of bisubstrate analogs with protein N-terminal methyltransferase 1 (NTMT1) were examined to probe the molecular properties of the NTMT1 active site through biochemical characterization and structural studies. Our results indicate that a 2-C to 4-C atom linker enables its respective bisubstrate analog to occupy both substrate and cofactor binding sites of NTMT1, but the bisubstrate analog with a 5-C atom linker only interacts with the substrate binding site and functions as a substrate. Furthermore, the 4-C atom linker is the optimal and produces the most potent inhibitor ($K_{i,\ app}$ = 130 ± 40 pM) for NTMT1 to date, displaying 400-fold selectivity over other methyltransferases and even to its homolog NTMT2. This study reveals the molecular basis for the plasticity of the NTMT1 active site. Additionally, we outline a general guidance on the development of bisubstrate inhibitors for any methyltransferases.

Introduction

Protein methylation, a widespread epigenetic modification that is catalyzed by protein methyltransferases (PMTs), plays critical roles in many cellular processes such as gene expression, transcriptional regulation, DNA replication and damage repair. Dysregulation of PMT expression has been implicated in a variety of diseases including cancer, cardiovascular, neurodegenerative, and other diseases.[1]–[5] Therefore, there have been emerging interests in development of selective inhibitors for PMTs as potential therapeutic agents. Recently, several inhibitors of PMTs have been developed and entered human clinical trials, such as DOT1-like protein inhibitor EPZ-5676 (Phase I/II), protein arginine methyltransferase 5 inhibitor GSK3326595 (Phase I/II), enhancer of zeste homolog 2 inhibitors EPZ-6438 (Phase I/II) and CPI-1205 (Phase I/II).[2]

PMTs utilize the cofactor S-adenosyl-L-methionine (SAM) as a methyl donor to transfer the methyl group from SAM onto the substrate with concomitant generation of S-adenosine-L-homocysteine (SAH) and methylated substrate.[2] The PMT-catalyzed methylation reaction typically undergoes a Bi-Bi mechanism and involves the formation of a ternary complex.[6] Bisubstrate analogs that occupy both substrate and cofactor binding sites have the potential to achieve higher binding affinities than a substrate analog.[7]–[9] Furthermore, bisubstrate analogs may offer superior selectivity for their targeted enzyme.[7],[10],[11] On account of a shared SAM cofactor binding pocket across PMT families, it is rational to hypothesize that bisubstrate analogs can be a general approach to offer potent and specific inhibitors for each individual PMT. Recent progresses have been made in the development of bisubstrate analogs for a few PMTs, such as protein N-terminal methyltransferase 1 (NTMT1)[10],[12],[13], coactivator-associated arginine methyltransferase 1 (CARM1)[14], protein arginine methyltransferase 1 (PRMT1)[15], and PRMT6. These bisubstrate analogs were created by connecting a SAM analog to a substrate or a functional group of the corresponding substrate. However, the potency of those bisubstrate analogs for their respective targets varied from nanomolar to micromolar. This serendipitous potency imposed the need of explicit instruction on design of bisubstrate analogs for PMTs.

The aforementioned need has prompted us to investigate how the linker length would affect the interaction of bisubstrate analog to its target PMT. Here, we used NTMT1 as a model system to examine the optimal length

of the linker, with the intention to provide a general guide to facilitate the design of optimal bisubstrate analogs for other PMTs. NTMT1 recognizes a unique X-P-K/R motif at the protein alpha-N-terminus.[16]-[18] It methylates centromere-specific histone H3 variants centromere protein A/B, regulator of chromatin condensation 1, damaged DNA-binding protein 2 and poly(ADP-ribose) polymerase 3.[19]-[24] Hence, NTMT1 has been implicated in regulating chromosome segregation, mitosis, and DNA damage repair.[20],[22],[25] We have previously developed bisubstrate analogs for NTMT1. Among them, compound NAH-C3-PPKRIA showed an IC_{50} value of 35 ± 2 nM in a MALDI-MS based assay, and displayed more than 100-fold selectivity against other methyltransferases (Figure 1A).[10] In addition, compound NAH-C3-GPRRRS showed an IC_{50} value of 0.94 ± 0.16 μM for NTMT1.[13] Both compounds have a propylene linker, which raises the question if a propylene linker is optimal. To address this question, we design and synthesize a series of NTMT1 bisubstrate analogs with variable linker lengths to probe the active site of NTMT1.

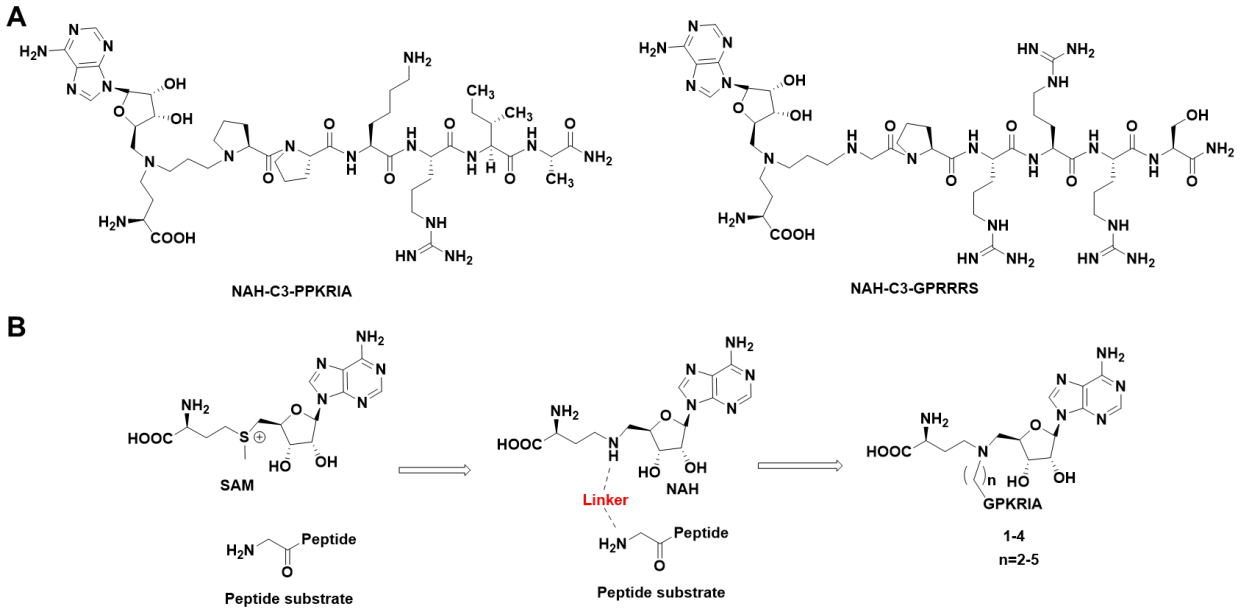

Figure 1. (A) Chemical structures of NTMT1 inhibitors. (B) Design of the bisubstrate analogs for NTMT1.

Results and Discussion

The linear distance between the sulfur atom of SAH and the nitrogen atom of substrate ranges 4.6 Å to 5.5 Å in the ternary structures of NTMT1.[16],[17] Therefore, we varied the linker from 2 to 5 methylene groups (Figure 1B,

Scheme 1). We chose the peptide GPKRIA due to the synthetic versatility of Gly at the first position. Compounds **1**-**4** were synthesized in a convergent manner by reacting the primary amines **8-11** with α-bromo peptide on resin and followed by acid treatment (Scheme 1).[13]

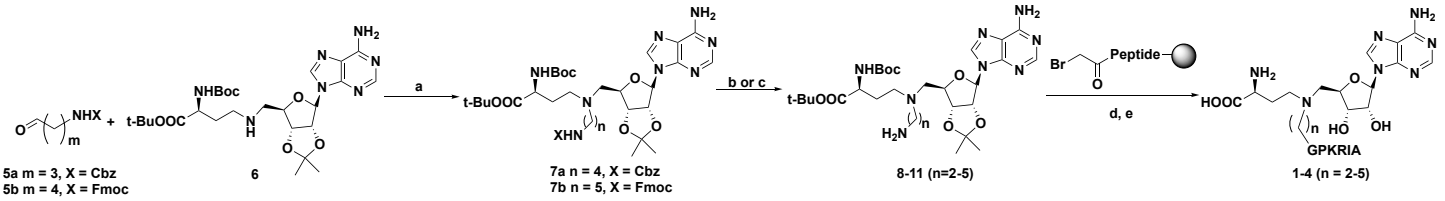

Scheme 1. Synthetic route for compounds 1-11. Reagents and conditions: a) $NaBH_3CN$, CH_3OH, r.t., 38-68%; b) 10% Pd/C, H_2, MeOH, 56%; c) DBU, CH_3CN, 0 °C to r.t., 71%; d) α-bromo peptides, DIPEA, DMF, r.t.; e) TFA: DODT: H_2O: TIPS = 94: 2.5: 2.5: 1; f) TFA, CH_2Cl_2, 0 °C to r.t., 42%; g) 4N HCl in dioxane, H_2O, 0 °C to r.t., 45%.

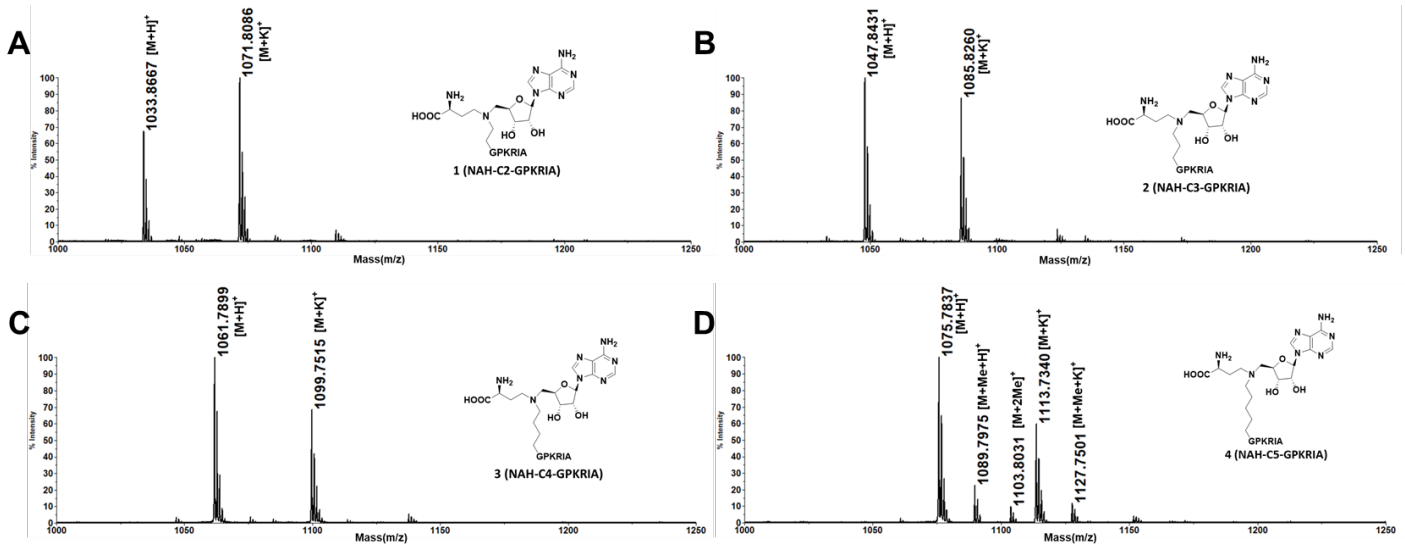

Figure 2. MALDI-MS methylation assay for the bisubstrate analogs **1**-**4**.

Compounds **1**-**4** were first subject to methylation assay catalyzed by NTMT1 in the presence of SAM to first check if they may act as possible substrates. Surprisingly, compound **4** containing the 5-C atom linker was able to be methylated by NTMT1 (Figure 2), indicating **4** as a substrate for NTMT1. Then, the inhibitory activities of **1**-**3** were evaluated in the SAH hydrolase (SAHH)-coupled fluorescence assay with 10 minutes of preincubation time.[32] Both SAM and the peptide substrate GPKRIA were at their respective K_m values. In order to

compare the inhibition activities of NAH-GPKRIA series under the same condition, we resynthesized and purified compounds **1** and **2** with an ethylene and a propylene linker, respectively. Their IC_{50} values were lower than previous values[13], which may be caused by an improved S/N ratio with a different GPKRIA peptide substrate and fluorescent dye ThioGlo4. The measured IC_{50} values for most compounds converged to the enzyme concentration (100 nM) present in the assay (Table 1), suggesting tight-binding inhibition. Therefore, using Morrison's equation to define their apparent K_i values is a better method to analyze the concentration-response data for these tight binding inhibitors.[33],[34] The tight-binding inhibitors often exhibit slow binding traits, but Morrison's equation applies to the steady state velocity.[33],[34] Therefore, the top inhibitor **3** was chosen to investigate the effects of preincubation time on the inhibitory activity of tight-binding inhibitors. The $K_{i,\ app}$ value of **3** was inversely proportional to the pre-incubation time (Figure 3A-B), indicating its slow binding feature. After 120 min pre-incubation, the $K_{i,app}$ value of **3** reached 130 ± 40 pM (Figure 3B), further substantiating its slow and tight binding feature ($[E]/K_{i,\ app} > 100$).[33],[34] Although the interaction between compound **3** and NTMT1 almost reached equilibrium after 30 min of incubation, subsequent inhibition studies were performed with 120 min of pre-incubation to make sure the equilibration reach steady state (Table 1). For the NAH-GPKRIA series, compound **3** containing a 4-C atom linker displayed the lowest $K_{i,app}$ value and best inhibition activity (Table 1). When the linker length decreased from a 4-C atom to a 3-C and 2-C, compound **2** ($K_{i,app}$ = 1.3 ± 0.6 nM) and **1** ($K_{i,app}$ = 5.4 ± 2.6 nM) exhibited a 10-fold and 40-fold decrease in comparison with **3**, respectively. The above results infer decent plasticity in the transition state of NTMT1 to accommodate linker length from 2-C to 4-C atom. Among them, a 4-C atom linker is the optimal length to achieve the best inhibition. Notably, a 5-C atom linker would convert a tight-binding bisubstrate analog to a substrate for NTMT1 (Figure 2).

The binding affinities of the bisubstrate compounds **1**-**4** for both NTMT1 and NTMT2 were determined by isothermal titration calorimetry (ITC) experiment to assess the selectivity between these two closely-related homolog isoforms that share over 50% sequence similarity and the same X-P-K recognition motif (Table 1).[35] All four compounds bound to NTMT1, especially compound **3** ($K_{d1/d2}$ = 0.6/0.3 μM). Notably, the K_d values of bisubstrate analogs were much higher than their $K_{i,app}$ values except compound **4**. This difference may be caused by endogenous amounts of SAM/SAH binding to recombinant NTMTs as reported before.[16],[35] However, the ITC

binding data was still informative, since the bisubstrate analogs at 1 mM showed negligible interactions with NTMT2.[35] This delicate selectivity further corroborates the benefits of bisubstrate analogs on account of their high specificity.

Table 1. NTMT inhibition evaluation and binding affinitis of NAH-GPKRIA bisubstrate analogs

Compound ID	IC_{50} (nM) [a, c]	$K_{i,app}$ (nM) [b, d]	$K_{d1/d2}$ for NTMT1 (μM)	$K_{d1/d2}$ for NTMT2 (μM)
1 (NAH-C2-GPKRIA)	260±70	5.4 ± 2.6	7/2	N.D.
2 (NAH-C3-GPKRIA)	130±40	1.3 ± 0.6	67/3	N.D.
3 (NAH-C4-GPKRIA)	82±17	0.13 ± 0.04	0.6/0.3	N.D.
4 (NAH-C5-GPKRIA)	N.A.	N.A.	3	N.D.

[a] IC_{50}s were determined with 10 min of preincubation time. [b] Morrison $K_{i,app}$ values are analyzed by the Morrison equation; [c] The values of IC_{50} for all compounds were determined with triplicate experiments (n = 3); [d] The values of $K_{i,app}$ for all compounds were determined with duplicate experiments (n = 2). N.A.: not applied. N.D.: no data.

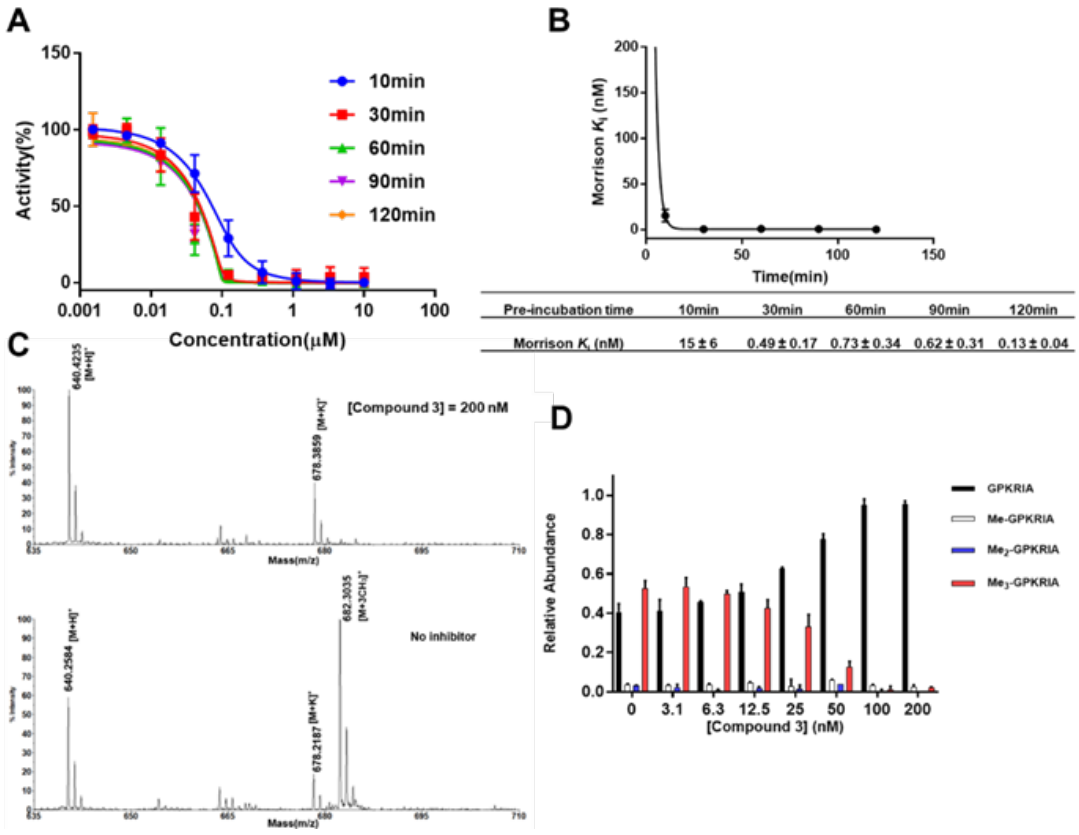

Pre-incubation time	10min	30min	60min	90min	120min
Morrison K_i (nM)	15 ± 6	0.49 ± 0.17	0.73 ± 0.34	0.62 ± 0.31	0.13 ± 0.04

Figure 3. (A) and (B) Time-dependent inhibition study of compound **3**. All experiments were run with duplicate (n=2), except 10min of pre-incubation (n=3). (A) Concentration–response plots for different pre-incubation times fitted to Morrison's quadratic equation for compound **3**; (B) Nonlinear regression of Morrison $K_{i,app}$ values with pre-incubation time. (C) and (D) MALDI-MS methylation inhibition assay compound **3** (n=2). (C) MALDI-MS results of MALDI-MS methylation inhibition assay for compound **3**; (D) Quantification of methylation progression of GPKRIA by NTMT1 with **3** at 20 min.

To further confirm the inhibitory activity of bisubstrate inhibitor, the MALDI-MS methylation assay was performed as an orthogonal assay to monitor the production of methylated peptides with both substrate peptide GPKRIA and SAM at their K_m values after 10 min of preincubation time (Figure 3C-D). At 50 nM of compound **3**, tri-methylation of GPKRIA peptide was substantially reduced. At 200 nM of compound **3**, tri-methylation of GPKRIA peptide was barely detected (Figure 3D).

The selectivity of **3** for NTMT1 was also examined against a panel of methyltransferases that shared a SAM binding pocket, which also included the coupling enzyme SAHH that has a SAH binding site and was used in the

fluorescence assay (Table 2, Figure S1). The compound barely showed inhibitory activity over euchromatic histone-lysine N-methyltransferase 2 (G9a), SET domain-containing protein 7 (SETD7) and nicotinamide N-methyltransferase (NNMT) at 100 μM. At 33 μM, **3** demonstrated less than 50% inhibition over protein arginine methyltransferase 1 (PRMT1), protein arginine methyltransferase 3 (PRMT3), *Trypanosoma brucei* protein arginine methyltransferase 7 (*Tb*PRMT7) and SAHH. Therefore, compound **3** showed more than 400-fold selectivity over other methyltransferases.

Table 2. Selectivity evaluation of compound 3

Enzyme activity (%) [a]	[**3**] (μM)				IC_{50}(μM)
	3.7	11	33	100	
G9a	95	94	88	78	>100
SETD7	101	106	101	86	>100
PRMT1	98	93	78	47	>33
PRMT3	98	87	58	26	>33
*Tb*PRMT7	93	82	60	30	>33
NNMT	99	97	97	93	>100
SAHH	84	71	57	40	>33

[a] The values of enzyme activity are mean values of duplicate experiments (n = 2).

To understand the molecular basis of the effect of different linkers, we obtained the co-crystal structures of bisubstrate analogs **1** and **4** with NTMT1 (Figure 4). The binary complex X-ray crystal structure of NTMT1-**1** complex (PDB: 6WJ7) illuminates the inhibition mechanism since compound **1** does occupy both cofactor and substrate binding sites of NTMT1. It also overlays well with previously reported bisubstrate inhibitor **NAH-C3-PPKRIA** in the X-ray crystal structure of NTMT1-**NAH-C3-PPKRIA** (PDB code: 6DTN) (Figure 4B). The SAM analog moiety of **1** in the binary complex binds almost same as **NAH-C3-PPKRIA**, which is nearly identical with SAH in the ternary complex of substrate peptide/SAH with NTMT1. When increasing the carbon linker to 5-C atom linker, the peptide part of the compound **4** retained its interaction with the substrate binding pocket and overlays very well with the PPKRIA peptide portion of **NAH-C3-PPKRIA** (Figure 4D-E). However,

the NAH moiety of the compound **4** no longer occupied the SAM binding pocket. The co-crystal structure of **4** in complex with NTMT1 (PDB: 6PVB) manifested that extending the linker to a 5-C atom linker may cause tension to prevent the bisubstrate analog from engaging with both binding sites. Interestingly, the SAM analog part inserted to a new pocket adjacent to the substrate binding pocket, which resulted in exposure of the secondary amine (α-N-terminal amine of the peptide portion) of compound **4** to receive the methyl group from SAM. Nevertheless, it infers the length of 5-C atom linker is too long to allow the bisubstrate analog **4** to simultaneously occupy both SAM and peptide binding sites.

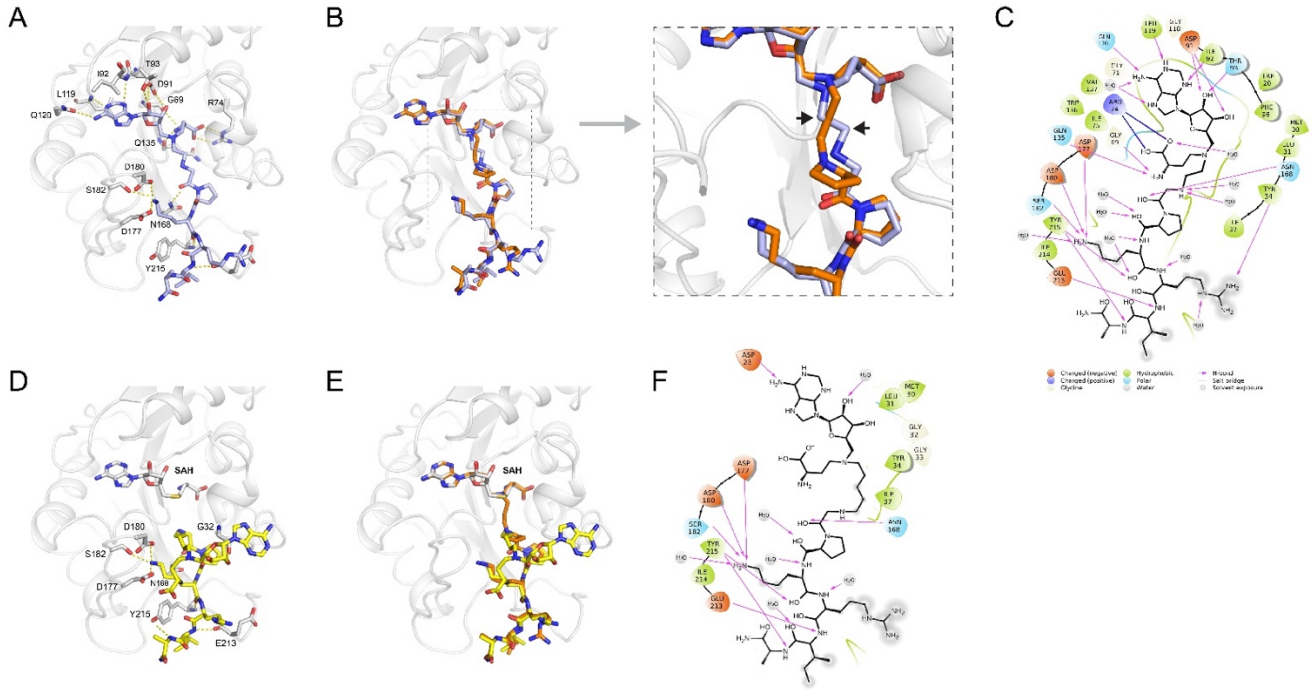

Figure 4. X-ray co-crystal structures. (A) The X-ray crystal structure of compound **1** (purple stick) in complex with NTMT1 (gray ribbon) (PDB code 6WJ7). H-bond interactions are shown in yellow dotted lines; (B) Overlay of the crystal structure of NTMT1(gray ribbon)-**1** (purple stick) complex with the crystal structure of the NTMT1-NAH-C3-PPKRIA (orange stick) binary complex (PDB code 6DTN); (C) Compound **1** 2D interaction diagram (Schrödinger Maestro) with NTMT1; (D) The X-ray crystal structure of NTMT1(gray ribbon)-**4** (yellow stick)-SAH (gray stick) (PDB code 6PVB). H-bond interactions are shown in yellow dotted lines; (E) Overlay of the crystal structure of NTMT1(gray ribbon)-**4** (yellow stick) - SAH (gray stick) complex (PDB code 6PVB) with the crystal structure of NTMT1-NAH-C3-PPKRIA (orange stick) binary complex (PDB code 6DTN).

Conclusion

In summary, a series of new bisubstrate analogs was designed and synthesized to probe the optimal linker length to develop potent and selective bisubstrate inhibitors for NTMT1, as well as provide insights into the transition state of PMTs. Inhibitory activities of bisubstrate analogs with a 2-C to 4-C atom linker infer astounding plasticity within the active site of NTMT1. Given the transient nature of transition state, these bisubstrate analogs serve as valuable tools to provide dynamic snapshots of the reorganization at the NTMT1 active site. Furthermore, top inhibitor **3** (NAH-C4-GPKRIA) containing a 4-C atom linker showed picomolar inhibition ($K_{i,\,app}$ = 130 ± 40 pM) for NTMT1, and more than 400-fold selectivity over other MTases including its close homolog NTMT2. Such delicate selectivity further corroborates the advantage of bisubstrate analogs to offer tight and selective inhibitors for individual target. However, increasing the carbon linker length to a 5-C atom resulted in a substrate instead of an inhibitor for NTMT1, which defined the scope or limit of plasticity. To our knowledge, this is the first case that delineates the optimal linker range of MTase bisubstrate analog and provide the molecular basis for the obliterated activity for longer linkers. The linear distance between the sulfonium ion and the nitrogen atom that accepting methyl group is very similar for most PMTs, which ranges from 3.5 Å to 5.5 Å among the ternary complex of all examined PMTs including NTMT1, SET domain-containing protein 8, and euchromatic histone-lysine N-methyltransferase 1.[16],[17],[26]–[29] Therefore, we propose that a 3-C or 4-C atom linker would serve as a general and feasible starting point to build bisubstrate analogs for any MTase. The optimal linker length has also been corroborated by successful inhibitors for RNA MTase, as a 3-C atom linker showed better inhibition compared to a 2-C atom linker.[36] Future directions will focus on applying such linkers to conjugate small molecule inhibitors that target individual binding sites to achieve higher selectivity and cell-potency.

Acknowledgements

We appreciate Dr. Darrel L. Peterson for purification of SAHH. We thank Krystal Diaz for purifying *Tb*PRMT7. The authors acknowledge the support from NIH grants R01GM117275 (RH), 1R01GM127896 (NN), 1R01AI127793 (NN), and P30 CA023168 (Purdue University Center for Cancer Research). The SGC is a registered charity (number 1097737) that receives funds from AbbVie, Bayer Pharma AG, Boehringer Ingelheim,

Canada Foundation for Innovation, Eshelman Institute for Innovation, Genome Canada through Ontario Genomics Institute [OGI-055], Innovative Medicines Initiative (EU/EFPIA) [ULTRA-DD grant no. 115766], Janssen, Merck KGaA, Darmstadt, Germany, MSD, Novartis Pharma AG, Ontario Ministry of Research, Innovation and Science (MRIS), Pfizer, São Paulo Research Foundation-FAPESP, Takeda, and Wellcome. We also thank supports from the Department of Medicinal Chemistry and Molecular Pharmacology (RH) and Department of Biological Sciences (NN) at Purdue University.

Author Information

Corresponding Author

*Phone: (765) 494 3426. E-mail: huang-r@purdue.edu

ORCID

Rong Huang: 0000-0002-1477-3165

Keywords: inhibitors • structure elucidation • bisubstrate analogs • methyltransferases • epigenetics

References

[1] S. M. Wang, D. H. Dowhan, G. E. O. Muscat, *J. Mol. Endocrinol.* **2019**, *62*, R223-7.

[2] H. U. Kaniskan, M. L. Martini, J. Jin, *Chem. Rev.* **2018**, *118*, 989-1068.

[3] W. Tsai, S. Niessen, N. Goebel, J. R. Yates, E. Guccione, M. Montminy, *Proc. Natl. Acad. Sci.* **2013**, *110* , 8870-8875.

[4] X. Liu, L. Wang, H. Li, X. Lu, Y. Hu, X. Yang, C. Huang, D. Gu, *Atherosclerosis* **2014**, *233*, 349–356.

[5] M. Luo, *Chem. Rev.* **2018**, *118*, 6656–6705.

[6] S. L. Richardson, Y. Mao, G. Zhang, P. Hanjra, D. L. Peterson, R. Huang, *J. Biol. Chem.* **2015**, *290*, 11601–11610.

[7] K. Parang, P. A. Cole, *Pharmacol. Ther.* **2002**, *93*, 145–157.

[8] E. M. Khalil, P. A. Cole, *J. Am. Chem. Soc.* **1998**, *7863*, 6195–6196.

[9] M. Yu, M. L. B. Magalha, P. F. Cook, J. S. Blanchard, *Biochemistry* **2006**, *45*, 14788–14794.

[10] D. Chen, G. Dong, N. Noinaj, R. Huang, *J. Med. Chem.* **2019**, *62*, 3773–3779.

[11] K. R. Brandvold, S. M. Santos, M. E. Breen, E. J. Lachacz, M. E. Steffey, M. B. Soellner, *ACS Chem. Biol.* **2015**, *10*, 1387–1391.

[12] G. Zhang, S. L. Richardson, Y. Mao, R. Huang, *Org. Biomol. Chem.* **2015**, *13*, 4149–4154.

[13] G. Zhang, R. Huang, *RSC Adv.* **2016**, *6*, 6768–6771.

[14] M. J. Van Haren, N. Marechal, N. Troffer-charlier, A. Cianciulli, G. Sbardella, J. Cavarelli, N. I. Martin, *Proc. Natl. Acad. Sci.* **2017**, 114, 3625-3630.

[15] T. Osborne, R. L. W. Roska, S. R. Rajski, P. R. Thompson, *J. Am. Chem. Soc.* **2008**, *130*, 4574-4575.

[16] C. Dong, Y. Mao, W. Tempel, S. Qin, L. Li, P. Loppnau, R. Huang, J. Min, *Genes Dev.* **2015**, *29*, 2343-2348.

[17] R. Wu, Y. Yue, X. Zheng, H. Li, *Genes Dev.* **2015**, *29*, 2337–2342.

[18] J. J. Petkowski, C. E. S. Tooley, L. C. Anderson, I. a Shumilin, J. L. Balsbaugh, D. F. Hunt, W. Minor, I. G. Macara, *Biochemistry* **2012**, *51*, 5942–5950.

[19] K. M. Dorgan, W. L. Wooderchak, D. P. Wynn, E. L. Karschner, J. F. Alfaro, Y. Cui, Z. S. Zhou, J. M. Hevel, *Anal. Biochem.* **2006**, *350*, 249–255.

[20] A. O. Bailey, T. Panchenko, K. M. Sathyan, J. J. Petkowski, P.-J. Pai, D. L. Bai, D. H. Russell, I. G. Macara, J. Shabanowitz, D. F. Hunt, B. E. Black, D. R. Foltz, *Proc. Natl. Acad. Sci.* **2013**, *110*, 11827–11832.

[21] X. Dai, K. Otake, C. You, Q. Cai, Z. Wang, H. Masumoto, Y. Wang, *J. Proteome Res.* **2013**, *12*, 4167–4175.

[22] Q. Cai, L. Fu, Z. Wang, N. Gan, X. Dai, Y. Wang, *J. Biol. Chem.* **2014**, *289*, 16046–16056.

[23] X. Dai, S. L. Rulten, C. You, K. W. Caldecott, Y. Wang, *J. Proteome Res.* **2015**, *14*, 2575–2582.

[24] C. E. S. Tooley, J. J. Petkowski, T. L. Muratore-Schroeder, J. L. Balsbaugh, J. Shabanowitz, M. Sabat, W. Minor, D. F. Hunt, I. G. Macara, *Nature* **2010**, *466*, 1125–1128.

[25] L. A. Bonsignore, J. G. Tooley, P. M. Van Hoose, E. Wang, A. Cheng, M. P. Cole, C. E. Schaner Tooley, *Mech. Ageing Dev.* **2015**, *146–148*, 42–52.

[26] P. A. Del Rizzo, L. M. A. Dirk, B. S. Strunk, M. S. Roiko, J. S. Brunzelle, R. L. Houtz, R. C. Trievel, *J. Biol. Chem.* **2010**, *285*, 31849–31858.

[27] S. Chuikov, J. K. Kurash, J. R. Wilson, B. Xiao, N. Justin, G. S. Ivanov, K. Mckinney, P. Tempst, C. Prives, S. J. Gamblin, N. A. Barlev, D. Reinberg, *Nature* **2004**, *432*, 353-360.

[28] J. Couture, E. Collazo, J. S. Brunzelle, R. C. Trievel, *Genes Dev.* **2015**, *19*, 1455–1465.

[29] H. Wu, J. Min, V. V. Lunin, T. Antoshenko, L. Dombrovski, H. Zeng, A. Allali-Hassani, V. Campagna-Slater, M. Vedadi, C. H. Arrowsmith, A. N. Plotnikov, M. Schapira, *PLoS One* **2010**, *5*, e8570.

[30] S. Nitrone, D. Keirs, D. Moffat, K. Overton, *J. Chem. Soc., Chem. Commun.* **1988**, 654-655

[31] M. Nasopoulou, D. Georgiadis, M. Matziari, V. Dive, G. Y. V Cedex, *J. Org. Chem.* **2007**, *72*, 7222-7228.

[32] A. Allali-hassani, G. A. Wasney, A. Siarheyeva, T. Hajian, M. Vedadi, H. Cheryl, *J. Biomol. Screen.* **2016**, *17*, 71-84.

[33] J. F. Morrison, *Trends Biochem. Sci.* **1982**, *7*, 102–105.

[34] R. A. Copeland, *Evaluation of Enzyme Inhibitors in Drug Discovery: A Guide for Medicinal Chemists and Pharmacologists*, 2nd Ed., Hoboken, New Jersey, **2013**.

[35] C. Dong, G. Dong, L. Li, L. Zhu, W. Tempel, Y. Liu, R. Huang, J. Min, *Commun. Biol.* **2018**, *1*, 1–9.

[36] S. Oerum, M. Catala, C. Atdjian, F. Brachet, P. Barraud, L. Iannazzo, L. Droogmans, M. Ethève-quelquejeu, C. Tisné, *RNA Biol.* **2019**, *16*, 798–808.

Table of Contents

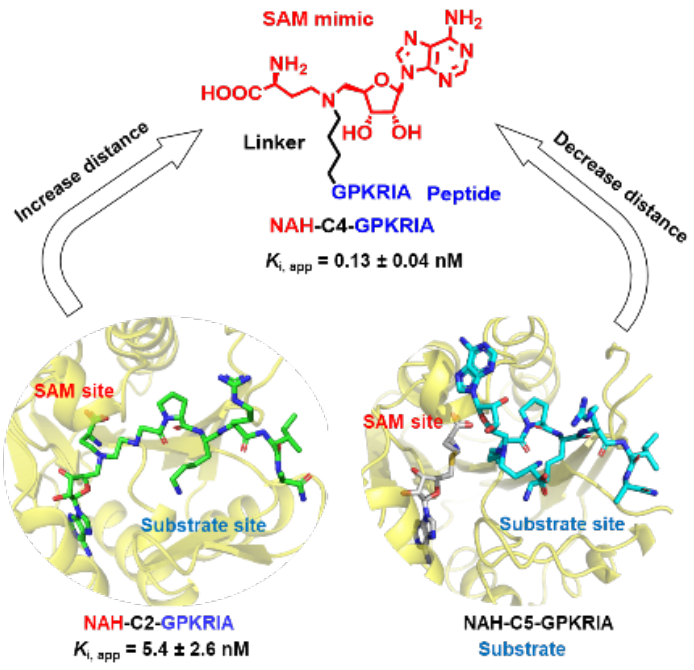

A series of bisubstrate analogs were examined to probe the protein N-terminal methyltransferase 1 (NTMT1) active site through biochemical characterization and structural studies. A 4-C atom linker yields the most potent bisubstrate inhibitor for NTMT1, while a 5-C atom linked bisubstrate analog functions as a substrate instead of an inhibitor.